DALTON
FULL PAPER

Crystal structures and vibrational and solid-state (CPMAS) NMR spectroscopy of some bis(triphenylphosphine)silver(I) sulfate, selenate and phosphate systems

Graham A. Bowmaker,*[a] John V. Hanna,*[b] Clifton E. F. Rickard[a] and Andrew S. Lipton[c]

[a] *Department of Chemistry, University of Auckland, Private Bag 92019, Auckland, New Zealand*
[b] *ANSTO NMR Facility, Materials Division, Private Mail Bag 1, Menai, N.S.W. 2234, Australia*
[c] *Environmental Molecular Sciences Laboratory, Pacific Northwest National Laboratory, Richland, Washington 99352, USA*

Received 26th September 2000, Accepted 8th November 2000
First published as an Advance Article on the web 7th December 2000

The crystal structures of $[Ag_2(PPh_3)_4(EO_4)]\cdot 2H_2O$ (E = S **1** or Se **2**) showed that these contain $[Ag_2(PPh_3)_4(EO_4)]$ units with three-coordinate silver and EO_4^{2-} bridging the two silver atoms *via* two oxygen atoms. The complexes $[Ag(PPh_3)_2(HEO_4)]\cdot H_2O$ (E = S **3** or Se **4**) contain $[Ag(PPh_3)_2(HEO_4)]$ molecules in which HEO_4^- is terminally bound to the silver atoms by a single oxygen atom. The complex $[Ag(PPh_3)_2(H_2PO_4)]\cdot 2EtOH$ **5** contains $[Ag(PPh_3)_2(H_2PO_4)]$ molecules in which $H_2PO_4^-$ is terminally bound to the silver atom, which is essentially three-coordinate. Heteronuclear $^1J(^{107/109}Ag,^{31}P)$ and homonuclear $^2J(^{31}P,^{31}P)$ spin–spin coupling constants for these compounds were determined by analysis of their high- (9.40 T) and very high-field (17.62 T) ^{31}P CPMAS NMR spectra, with the aid of the 2-D ^{31}P CPCOSY technique, and a strong inverse correlation was found between $^1J(^{107/109}Ag,^{31}P)$ and the Ag–P bond length. IR and Raman studies show that the effect of a bound proton on the vibrational frequencies of EO_4^{2-} is much greater than that of an attached metal atom.

Introduction

The many structural studies of silver(I) complexes that have been reported demonstrate the structural versatility of silver(I) in its coordination chemistry.[1,2] Many of these complexes involve anionic ligands such as halides, pseudohalides and oxyanions. Some types of oxyanion complex, such as those involving carboxylate ligands, have been known for a long time,[3,4] and we have recently characterized a number of such complexes by structural and spectroscopic methods.[5,6] In the course of this work our attention was drawn to the fact that relatively little is known about the structures and properties of silver(I) complexes involving simple multiply charged inorganic anions such as sulfate or phosphate. Such ions can be coordinated in the fully deprotonated form (*e.g.* SO_4^{2-}) or in a protonated form (*e.g.* HSO_4^-). A structure reported some years ago for the silver(III) complex $[Ag(C_6H_{16}N_{10})]SO_4[HSO_4]\cdot H_2O$ ($C_6H_{16}N_{10}$ = ethylenebis(biguanide)) reveals the presence of monodentate SO_4^{2-} and HSO_4^- in the same molecule, with the somewhat unexpected result that the Ag–O distance for SO_4^{2-} is greater than that for HSO_4^-.[7] A few silver complexes involving SO_4^{2-} or HSO_4^- ligands have been reported,[8–11] most of which also contain N-donor ligands.[9–11] There have been no reports of such complexes with P-donor ligands. In the present work we report the preparation and structures of two such compounds and their selenate analogues, $[Ag_2(PPh_3)_4(EO_4)]\cdot 2H_2O$ (E = S **1** or Se **2**) and $[Ag(PPh_3)_2(HEO_4)]\cdot H_2O$ (E = S **3** or Se **4**). Also reported are similar results for $[Ag(PPh_3)_2(H_2PO_4)]\cdot 2EtOH$ **5**, which is related to **3** *via* the isoelectronic relationship between HSO_4^- and $H_2PO_4^-$. We have also studied these and some related compounds by vibrational and solid-state CPMAS NMR spectroscopy.

Vibrational spectroscopy is expected to provide information about the nature of the coordinated anion (*e.g.* whether protonated or not) and on its mode of coordination. This method is potentially useful in situations where such information cannot be obtained directly from single-crystal structure determinations. A situation of this kind occurs in the study of oxyanions adsorbed from aqueous solution onto a metal surface. A number of studies have indicated the existence of adsorbed sulfate, hydrogensulfate, phosphate, *etc.* at the surface of Group 11 metal electrodes.[12–18] In most of these studies the evidence for the state of protonation and the mode of bonding of the anion to the surface is indirect, and it is possible that the correlation between the vibrational spectra and the structures of well characterized coordination compounds involving the same anions and metal might provide a further means of characterizing the surface species. It is true that the coordination compounds studied here involve the metal in the formal +1 oxidation state, whereas the atoms in a bulk metal electrode formally have an oxidation state of zero. However, recent studies have shown that the oxidation states of surface metal atoms bound to the anionic adsorbate are close to +1,[13,15] so these two types of system may be more closely related than is apparent at first sight.

For the NMR investigations of these systems, low field (2.11 T) ^{13}C CPMAS studies and ^{31}P CPMAS studies at high field (9.40 T) and very high field (17.62 T) have been undertaken. The 100% natural abundance of the $I = 1/2$ ^{31}P isotope makes ^{31}P CPMAS NMR a particularly useful and sensitive technique. Previous ^{31}P CPMAS NMR studies of bis-silver phosphine systems have shown that each unique phosphorus site is characterized by both heteronuclear $^1J(^{107/109}Ag,^{31}P)$ and homonuclear $^1J(^{31}P,^{31}P)$ scalar (or spin–spin) couplings when chemical inequivalence between each phosphorus site exists.[5,6,19,20] In particular, the $^1J(Ag,P)$ coupling constant is a useful probe of the coordination of the metal centres within these complexes. In this case, each phosphorus position is represented as a doublet

 DOI: 10.1039/b007796h

of doublets with an intensity distribution governed by the chemical shift difference between the ^2J(P,P) coupled pairs and a A_2X, ABX or AMX spin system description is subsequently invoked. In the event that more than 2 inequivalent phosphorus sites exist in the unit cell, techniques such as 2-D ^{31}P CPCOSY at high field (9.40 T) have become an important tool for the disentanglement and correct assignment of the complex spectra that ensue.[6,19,20] However, when very small chemical shift separations exist between inequivalent ^2J(P,P) coupled sites (and A_2X or ABX spin systems are described), the use of 2-D techniques alone is not sufficient and data acquisition at significantly higher fields becomes necessary. The advent of very high field instrumentation operating at 17.62 and 18.80 T (*i.e.* ^{1}H frequencies of 750 and 800 MHz, respectively) partially relaxes the strongly coupled A_2X and ABX spin conditions that can dominate these ^{31}P multiplets at lower field strengths, thus facilitating more confident assignment and accurate measurement of spectral parameters. The results presented in this paper describe the first very high field ^{31}P CPMAS NMR study of any metal phosphine system and demonstrate the complementary nature of the emerging data to those acquired on more routinely accessed high field instrumentation.

Experimental

Preparation of compounds

$[Ag_2(PPh_3)_4(SO_4)]\cdot 2H_2O$ 1. A mixture of Ag_2SO_4 (0.31 g, 1.0 mmol) and PPh_3 (1.05 g, 4.0 mmol) was dissolved in boiling ethanol (10 ml). Water (5 ml) was added to the hot solution, which was allowed to stand in the air. The white crystalline product, which formed as the volume of the solution reduced to about 10 ml by evaporation, was collected and washed with ethanol. Yield 1.14 g (82%). Found: C 62.1, H 4.8%. Calc. for $C_{72}H_{64}Ag_2O_6P_4S$: C 61.9, H 4.6%.

$[Ag_2(PPh_3)_4(SeO_4)]\cdot 2H_2O$ 2. A mixture of Ag_2SeO_4 (0.36 g, 1.0 mmol) and PPh_3 (1.05 g, 4.0 mmol) was dissolved in boiling ethanol (10 ml). The resulting cloudy greyish green solution was filtered while hot to yield a colourless filtrate, and water (5 ml) added to the hot filtrate. The white crystalline product, which formed as the warm solution slowly cooled to room temperature, was collected and washed with ice-cold ethanol–water (2 : 1). Yield 1.12 g (78%). Found: C 60.0, H 4.5%. Calc. for $C_{72}H_{64}Ag_2O_6P_4Se$: C 59.9, H 4.5%.

$[Ag(PPh_3)_2(HSO_4)]\cdot H_2O$ 3. A mixture of Ag_2SO_4 (0.31 g, 1.0 mmol) and PPh_3 (1.05 g, 4.0 mmol) was dissolved in boiling ethanol (10 ml) to which 98% H_2SO_4 (0.11 g, 1.1 mmol) had been added. The clear solution was allowed to stand in the air. The white crystalline product, which formed as the volume of the solution reduced to about 5 ml by evaporation, was collected and washed with ice-cold ethanol. Yield 1.10 g (73%). Found: C 57.9, H 4.4%. Calc. for $C_{36}H_{33}AgO_5P_2S$: C 57.8, H 4.5%.

$[Ag(PPh_3)_2(HSeO_4)]\cdot H_2O$ 4. A mixture of Ag_2SeO_4 (0.36 g, 1.0 mmol) and PPh_3 (1.05 g, 4.0 mmol) was dissolved in warm ethanol (10 ml) until nearly all of the solids dissolved. On cooling, a white solid (probably $[Ag_2(PPh_3)_4(SeO_4)]$) separated. To this a solution of H_2SeO_4 (0.22 g, 1.5 mmol) in water (5 ml) was added and the mixture heated with stirring until the white solid just dissolved. The white crystalline product, which formed as the solution slowly cooled to room temperature, was collected and washed with ice-cold ethanol–water (1 : 1). Yield 1.33 g (84%). Found: C 54.7, H 4.2%. Calc. for $C_{36}H_{33}AgO_5P_2Se$: C 54.4, H 4.2%.

Ag_3PO_4. A solution of KH_2PO_4 (0.95 g, 7 mmol) and KOH (0.79g, 14 mmol) in water (20 ml) was added to a solution of $AgNO_3$ (3.57 g, 21 mmol) in water (10 ml). The resulting bright yellow precipitate was collected and washed with water, ethanol and diethyl ether. Yield 2.58 g (88%).

Ag_2HPO_4. A mixture of 90% H_3PO_4 (0.39 g, 3.6 mmol) and Ag_3PO_4 (0.84 g, 2.0 mmol) was placed in an oven at 90 °C for 1 h, whereupon the yellow Ag_3PO_4 turned creamy white. The mixture was treated with a little acetone and allowed to stand for 30 min at room temperature. The product was collected and washed with acetone. Yield 0.92 g (98%).

$[Ag(PPh_3)_2(H_2PO_4)]\cdot 2EtOH$ 5. A mixture of Ag_3PO_4 (0.1 g, 0.24 mmol) and PPh_3 (0.38 g, 1.43 mmol) was dissolved in ethanol (5 ml) to which 90% H_3PO_4 (0.06 g, 0.55 mmol) had been added. The clear solution was allowed to stand in the air. The white crystalline product, which formed as the volume of the solution reduced to about 3.5 ml by evaporation, was collected and washed with ice-cold ethanol. Yield 0.47 g (79%). Found: C 58.4, H 4.9%. Calc. for $C_{40}H_{44}AgO_6P_3$: C 58.5, H 5.4%.

Structure determinations

Spheres of X-ray data were collected using a Siemens SMART diffractometer with a CCD area detector system at 200 K. Monochromatic Mo-Kα radiation ($\lambda = 0.7107_3$ Å) was employed in all cases. Absorption corrections were applied semi-empirically by analysis of equivalents and equivalent reflections averaged to give the unique data sets. The structures were solved by direct methods and refined by full matrix least squares on F^2 after absorption corrections. Anisotropic thermal parameters were refined for the non-hydrogen atoms; (x, y, z, $U_{iso})_H$ were included constrained at estimated values. Neutral atom complex scattering factors were used. Conventional residuals R on $|F|$ and R_w on $|F|^2$ are quoted at convergence. Computation used SHELX 97.[21] The carbon atoms of the PPh_3 ligands are labelled C(lmn) where l is the ligand number, m the ring number 1, 2 or 3 and n the atom number 1–6 with the carbon bound to the phosphorus labelled C(lm1).

Crystal/refinement data. $[Ag_2(PPh_3)_4(SO_4)]\cdot 2H_2O$ **1** ≡ $C_{72}H_{64}Ag_2O_6P_4S$, $M = 1396.91$, triclinic, space group $P\bar{1}$ (C_i^1 no. 2), $a = 12.4953(4)$, $b = 13.3274(4)$, $c = 21.7824(6)$ Å, $\alpha = 91.1910(10)$, $\beta = 95.3060(10)$, $\gamma = 118.2300(10)°$, $V = 3173.6$ Å^3, $Z = 2$, $\mu = 8.04$ cm^{-1}, $N = 13366$, N_o ($I > 2\sigma(I)$) = 11528, $R = 0.048$, $R_w = 0.120$.

$[Ag_2(PPh_3)_4(SeO_4)]\cdot 2H_2O$ **2** ≡ $C_{72}H_{64}Ag_2O_6P_4Se$, $M = 1443.81$, triclinic, space group $P\bar{1}$ (C_i^1, No. 2), $a = 12.46450(10)$, $b = 13.2640(1)$, $c = 21.85890(10)$ Å, $\alpha = 91.5060(10)$, $\beta = 95.2500(10)$, $\gamma = 117.950(1)°$, $V = 3169.1$ Å^3, $Z = 2$, $\mu = 13.35$ cm^{-1}, $N = 13379$, N_o ($I > 2\sigma(I)$) = 11996, $R = 0.022$, $R_w = 0.053$.

$[Ag(PPh_3)_2(HSO_4)]\cdot H_2O$ **3** ≡ $C_{36}H_{33}AgO_5P_2S$, $M = 747.49$, triclinic, space group $P\bar{1}$ (C_i^1, no. 2), $a = 12.58420(10)$, $b = 13.26680(10)$, $c = 24.3057(3)$ Å, $\alpha = 92.9180(10)$, $\beta = 103.5360(10)$, $\gamma = 118.0230(10)°$, $V = 3420.9$ Å^3, $Z = 4$, $\mu = 7.84$ cm^{-1}, $N = 14368$, N_o ($I > 2\sigma(I)$) = 12199, $R = 0.034$, $R_w = 0.083$.

$[Ag(PPh_3)_2(HSeO_4)]\cdot H_2O$ **4** ≡ $C_{36}H_{33}AgO_5P_2Se$, $M = 794.39$, triclinic, space group $P\bar{1}$ (C_i^1, no. 2), $a = 12.5358(2)$, $b = 13.2580(2)$, $c = 24.5566(2)$ Å, $\alpha = 104.3870(10)$, $\beta = 91.6760(10)$, $\gamma = 117.4040(10)°$, $V = 3460.4$ Å^3, $Z = 4$, $\mu = 17.67$ cm^{-1}, $N = 14255$, N_o ($I > 2\sigma(I)$) = 11986, $R = 0.057$, $R_w = 0.117$.

$[Ag(PPh_3)_2(H_2PO_4)]\cdot 2EtOH$ **5** ≡ $C_{40}H_{44}AgO_6P_3$, $M = 821.53$, triclinic, space group $P\bar{1}$ (C_i^1, no. 2), $a = 10.10970(10)$, $b = 13.11210(10)$, $c = 16.00730(10)$ Å, $\alpha = 73.100(1)$, $\beta = 77.5550(10)$, $\gamma = 78.8890(10)°$, $V = 1963.2$ Å^3, $Z = 2$, $\mu = 6.80$ cm^{-1}, $N = 8235$, N_o ($I > 2\sigma(I)$) = 7452, $R = 0.024$, $R_w = 0.063$.

CCDC reference number 186/2267.

See http://www.rsc.org/suppdata/dt/b0/b007796h/ for crystallographic files in .cif format.

Spectroscopy

Infrared spectra were recorded at 4 cm^{-1} resolution at room temperature as Nujol mulls between KBr plates on a Perkin-Elmer Spectrum 1000 Fourier-transform infrared spectrometer. Far-infrared spectra were obtained with 2 cm^{-1} resolution at room temperature as pressed Polythene discs on a Digilab FTS-60 Fourier-transform infrared spectrometer employing an FTS-60V vacuum optical bench with a 5 lines mm^{-1} wire mesh beam splitter, a mercury lamp source and a pyroelectric triglycine sulfate detector. Raman spectra were recorded at 4.5 cm^{-1} resolution using a Jobin-Yvon U1000 spectrometer equipped with a cooled photomultiplier (RCA C31034A) detector. The 514.5 nm exciting line from a Spectra-Physics Model 2016 argon-ion laser was used.

Solid-state ^{31}P CPMAS NMR spectra were obtained at ambient temperature on Bruker MSL-400 (9.40 T) and Varian Inova-750 (17.62 T) spectrometers operating at ^{31}P frequencies of 161.92 and 303.53 MHz, respectively. Conventional cross-polarization[22] and magic-angle-spinning[23] techniques, coupled with spin temperature alternation[24] to eliminate spectral artifacts, were implemented using Bruker 4 mm (9.40 T) and Jakobsen 5 mm (17.62 T) double-air-bearing probes in which MAS frequencies of ≥10 kHz were achieved. A recycle delay of 15–30 s, Hartmann–Hahn contact period of 2–5 ms and a ^{1}H decoupling field of 80–85 kHz (during acquisition) were common to all ^{31}P spectra. For the 9.40 T experiments, the initial ^{1}H $\pi/2$ pulse width (prior to the Hartmann–Hahn match) was 3 μs, and at 17.62 T the initial ^{1}H $\pi/2$ pulse width was 6 μs. No spectral smoothing was employed prior to Fourier transformation. The 2-D ^{31}P CPCOSY experiment was implemented with the TPPI (time proportional phase incrementation) method[25] for acquisition of phase-sensitive data in both the F1 and F2 dimensions. The application of this technique has been discussed in detail elsewhere.[26] The recycle delay, contact period, ^{1}H $\pi/2$ pulse width and MAS rate were the same as those implemented in the above 1-D ^{31}P CPMAS experiments. A total of 256 F1 increments were acquired into 256 word blocks, with both dimensions zero-filled to 1 K words and weighted with Gaussian multiplication prior to Fourier transformation. All ^{31}P chemical shifts were externally referenced to triphenylphosphine which has a shift of δ −9.9 with respect to 85% H_3PO_4. Solid-state ^{13}C CPMAS NMR spectra were obtained at ambient temperature on a Bruker CXP-90 spectrometer operating at a ^{13}C frequency of 22.63 MHz. The cross-polarization methods outlined above were implemented on a Doty 7 mm probe in which MAS frequencies of 4 kHz were achieved. A recycle delay of 10 s, contact period of 5 ms and initial ^{1}H $\pi/2$ pulse width of 3.5 μs were common to all ^{13}C spectra. No spectral smoothing was employed prior to Fourier transformation, and ^{13}C chemical shifts were referenced to TMS *via* an external sample of solid hexamethylbenzene.

Results and discussion

The 1:2 silver(I) sulfate or selenate complexes with triphenylphosphine are readily prepared by reaction of stoichiometric quantities of the reagents in aqueous ethanol. The corresponding hydrogensulfate or hydrogenselenate complexes are obtained under similar conditions by addition of slightly more than the stoichiometrically required amount of the appropriate acid H_2EO_4 (E = S or Se) to the reaction mixture before crystallization, eqn. (1). If insufficient water is present in these reactions,

$$Ag_2EO_4 + 4PPh_3 + H_2EO_4 \longrightarrow 2[Ag(PPh_3)_2(HEO_4)] \quad (1)$$

products containing ethanol of solvation are sometimes obtained, but these are unstable with respect to loss of ethanol. When sufficient water is present the products are obtained as the stable hydrates **1**–**4**.

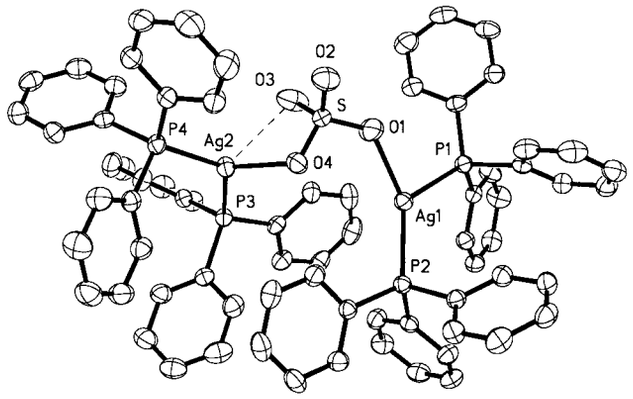

Fig. 1 Molecular structure of $[Ag_2(PPh_3)_4(SO_4)]\cdot 2H_2O$ **1** showing all non-hydrogen atoms and the atom numbering scheme. 50% Probability amplitude displacement ellipsoids are shown.

Table 1 Core geometries for $[Ag_2(PPh_3)_4(EO_4)]\cdot 2H_2O$ (E = S **1** or Se **2**)

	1 (E = S)	**2** (E = Se)
Ag(1)–P(1)	2.5018(11)	2.4994(4)
Ag(1)–P(2)	2.4190(11)	2.4105(5)
Ag(1)–O(1)	2.235(4)	2.2342(15)
Ag(2)–P(3)	2.4625(11)	2.4590(4)
Ag(2)–P(4)	2.4380(11)	2.4289(4)
Ag(2)···O(3)	2.643(4)	2.6507(16)
Ag(2)–O(4)	2.394(3)	2.4025(13)
E–O(1)	1.472(4)	1.6403(15)
E–O(2)	1.464(4)	1.6271(13)
E–O(3)	1.466(4)	1.6394(14)
E–O(4)	1.489(3)	1.6489(13)
P(1)–Ag(1)–P(2)	128.04(4)	128.353(16)
P(1)–Ag(1)–O(1)	92.81(11)	90.38(4)
P(2)–Ag(1)–O(1)	136.65(12)	138.40(5)
Ag(1)–O(1)–E	129.6(2)	127.94(8)
P(3)–Ag(2)–P(4)	128.60(4)	128.755(16)
P(3)–Ag(2)–O(3)	113.73(10)	112.73(4)
P(4)–Ag(2)–O(3)	112.04(10)	111.74(4)
P(3)–Ag(2)–O(4)	102.97(9)	100.36(4)
P(4)–Ag(2)–O(4)	121.36(9)	122.21(4)
O(3)–Ag(2)–O(4)	56.42(11)	62.46(4)
Ag(2)–O(3)–E	92.79(18)	91.17(6)
Ag(2)–O(4)–E	102.63(17)	100.18(6)

The 1:2 silver dihydrogenphosphate complex with triphenylphosphine was obtained by a reaction analogous to (1); eqn. (2). In this case the stable ethanol disolvate **5** was obtained from ethanol solution.

$$Ag_3PO_4 + 6PPh_3 + 2H_3PO_4 \longrightarrow 3[Ag(PPh_3)_2(H_2PO_4)] \quad (2)$$

Crystal structure determinations

The structure of $[Ag_2(PPh_3)_4(SO_4)]\cdot 2H_2O$ **1** is shown in Fig. 1. Its core geometries and those for the isomorphous selenium analogue **2** are given in Table 1. These compounds contain $Ag(PPh_3)_2$ units that are linked by a bridging EO_4 group, which coordinates to the two silver atoms in the dimer *via* the two oxygen atoms O(1) and O(4). The two silver atoms are essentially three-coordinate with almost planar environments, although there is a weak secondary Ag(2)···O(3) interaction that results in Ag(2)–O(4) being slightly longer than Ag(1)–O(1). The E–O bonds involving the oxygen atoms O(1) and O(4) in the primary coordination spheres of the two silver atoms are slightly longer than those involving O(2) and O(3). The Ag(1)–O(1) and Ag(2)–O(4) distances in the sulfate complex are shorter than those in most previously reported silver sulfate complexes, where the coordination number of silver ranges from three to six.[7,9–11] A shorter Ag–O of 2.18(4) Å has been reported in the 1:3 complex $[Ag_2L_3(SO_4)(H_2O)]$ (L = [1,2,4]-

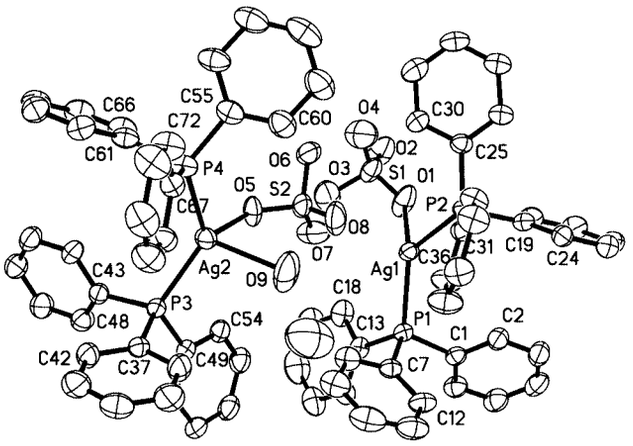

Fig. 2 Molecular structure of $[Ag(PPh_3)_2(HSO_4)]\cdot H_2O$ **3**. Details as for Fig. 1.

Table 2 Core geometries for $[Ag(PPh_3)_2(HEO_4)]\cdot H_2O$ (E = S **3** or Se **4**)

	3 (E = S)	**4** (E = Se)
Ag(1)–P(1)	2.4316(7)	2.4405(13)
Ag(1)–P(2)	2.4394(7)	2.4349(13)
Ag(1)–O(1)	2.410(2)	2.421(4)
Ag(2)–P(3)	2.4300(7)	2.4278(15)
Ag(2)–P(4)	2.4265(8)	2.4275(14)
Ag(2)–O(5)	2.412(2)	2.402(4)
Ag(2)–O(9)	2.446(3)	2.439(5)
E(1)–O(1)	1.431(2)	1.589(4)
E(1)–O(2)	1.436(2)	1.596(4)
E(1)–O(3)	1.538(3)	1.626(6)
E(1)–O(4)	1.472(3)	1.687(6)
E(2)–O(5)	1.441(2)	1.611(4)
E(2)–O(6)	1.532(2)	1.618(5)
E(2)–O(7)	1.470(3)	1.689(4)
E(2)–O(8)	1.450(3)	1.624(5)
P(1)–Ag(1)–P(2)	131.38(2)	131.13(5)
P(1)–Ag(1)–O(1)	113.72(8)	100.99(15)
P(2)–Ag(1)–O(1)	103.15(8)	113.66(15)
Ag(1)–O(1)–E(1)	133.14(14)	129.03(24)
P(3)–Ag(2)–P(4)	130.48(3)	131.20(5)
P(3)–Ag(2)–O(5)	108.28(6)	108.07(12)
P(4)–Ag(2)–O(5)	110.46(6)	108.19(11)
P(3)–Ag(2)–O(9)	107.32(11)	106.9(2)
P(4)–Ag(2)–O(9)	105.70(13)	105.66(19)
O(5)–Ag(2)–O(9)	84.92(10)	88.45(18)
Ag(2)–O(5)–E(2)	136.00(14)	129.76(21)

triazolo[1,5-*a*]pyrimidine) in which a four-coordinate silver atom is bound to a monodentate sulfate ligand and to three N atoms of three triazolopyrimidine ligands.[10] However, in the 1:2 complex $[Ag_2L_2(SO_4)(H_2O)]$, in which the sulfate bridges two four-coordinate silver atoms, Ag–O increases to 2.393(7), 2.556(7) Å.[10] The shorter Ag–O in the present sulfate (at Ag(1) in particular) is no doubt due at least in part to the smaller coordination number (three) in this compound.

All four PPh_3 ligands in complexes **1** and **2** are crystallographically inequivalent, and the degree of inequivalence as measured by the Ag–P bond lengths is almost identical for the E = S and Se compounds. This contrasts with the results of the ^{31}P CPMAS NMR study of these compounds (see below). The Ag–P bond lengths range from 2.41 to 2.50 Å and the P–Ag–P angles from 128.0 to 128.8°. The water molecules are hydrogen bonded to the EO_4 oxygen atoms, which are not bonded to Ag.

The structure of $[Ag(PPh_3)_2(HSO_4)]\cdot H_2O$ **3** is shown in Fig. 2. Its core geometries and those for the isomorphous selenium analogue **4** are given in Table 2. These compounds contain two distinct $Ag(PPh_3)_2(HEO_4)$ molecules in which the HEO_4^- groups are terminally bound to the two silver atoms Ag(1) and Ag(2) *via* O(1) and O(5) respectively. The structures

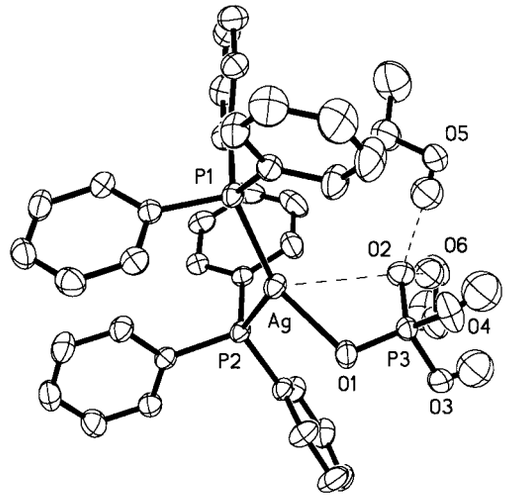

Fig. 3 Molecular structure of $[Ag(PPh_3)_2(H_2PO_4)]\cdot 2EtOH$ **5**. Details as for Fig. 1.

Table 3 Core geometries for $[Ag(PPh_3)_2(H_2PO_4)]\cdot 2EtOH$ **5**

Ag–P(1)	2.4309(4)	P(1)–Ag–O(1)	123.96(3)
Ag–P(2)	2.4595(4)	P(2)–Ag–O(1)	107.27(3)
Ag–O(1)	2.3280(12)	P(1)–Ag–P(2)	127.671(14)
P(3)–O(1)	1.5051(12)	P(3)–O(1)–Ag	103.77(6)
P(3)–O(2)	1.5169(13)		
P(3)–O(3)	1.5759(14)		
P(3)–O(4)	1.5759(14)		

of these two molecules are unexpectedly different. In one the silver atom Ag(1) is essentially three-coordinate with an almost planar environment, whereas in the other the silver atom Ag(2) is four-coordinate because this molecule also contains a bound water molecule, with Ag(2)–O(9) ≈ 2.45 Å. The non-bonded water molecule forms hydrogen bonds to the bonded water molecule and an oxygen of the HEO_4^- group of the three-coordinate silver atom and thus links the two parts together. Although the protons in the HEO_4^- groups are not located in the crystal structure determination, the fact that the E–O bonds involving the oxygen atoms O(3) and O(6) are significantly longer than the others suggests that the protons reside on these atoms. Despite the differences in the coordination environments in the two molecules, the Ag(1)–O(1) and Ag(2)–O(5) distances are not very different, with values of about 2.41 Å. This is slightly longer than the Ag–O distances involving the bridging sulfate in **1** and **2**. This is as expected, since the strongly bound proton in HEO_4^- should reduce the coordinating ability of this species relative to EO_4^{2-}. For comparison, Ag–O distances in the recently determined crystal structure of $AgHSO_4$ lie in the range 2.41–2.69 Å.[8] The P–Ag–P angles in **3** and **4** (*ca.* 131°) are slightly greater than those in **1** and **2** (*ca.* 128°), in agreement with the above conclusion that the Ag–O bonding involving HEO_4^- is weaker than that involving EO_4^{2-}.

The structure of $[Ag(PPh_3)_2(H_2PO_4)]\cdot 2EtOH$ **5** is shown in Fig. 3. The core geometry parameters are given in Table 3. This compound contains unique $Ag(PPh_3)_2(H_2PO_4)$ molecules in which the H_2PO_4 group is terminally bound to the silver atom *via* O(1). The silver atom is essentially three-coordinate with a very nearly planar environment. The protons in the $H_2PO_4^-$ group are located on O(3) and O(4), consistent with the fact that the P–O bonds involving these oxygen atoms are significantly longer than the others. The Ag–O(1) distance of 2.3280(12) Å is significantly shorter than the shortest Ag–O distances (*ca.* 2.41 Å) in the HEO_4^- complexes **3** and **4**, consistent with the fact that $H_2PO_4^-$ is a stronger base than HSO_4^- or $HSeO_4^-$. This is also reflected in fact that the P–Ag–P angle in **5** (*ca.* 128°) is smaller than those in **3** and **4** (*ca.* 131°). The solvate ethanol molecules in **5** are hydrogen bonded to the

phosphate oxygen atom O(2), with O(2)···O(5) 2.680(2) and O(2)···O(6) 2.688(2) Å. These distances are typical for weak hydrogen bonding.[27] There is also a possible weak interaction between Ag and O(2) [Ag···O(2) 2.838(1) Å].

Solid-state NMR spectroscopy

The solid-state ^{13}C CPMAS NMR spectra of complexes **1**–**4** exhibit only one broad unresolved resonance at δ *ca.* 130 due to the PPh_3 ligands. In addition, the spectrum of **5** shows further resonances at δ 18.0, 56.3 and 58.9 due to ethanol molecules of solvation. The last two signals are attributed to the CH_2 carbons on the two crystallographically inequivalent ethanol molecules.

The solid-state ^{31}P CPMAS NMR spectra and 2-D ^{31}P CPCOSY spectra of complexes **1**–**5** are shown in Figs. 4 and 5, respectively. In general, the spectra consist of partially resolved multiplets due to the individual ^{31}P chemical shifts emanating from the chemically inequivalent phosphorus nuclei bound to each Ag. Each resonance displays $^1J(^{107,109}Ag,^{31}P)$ scalar coupling between the ^{31}P ($I = 1/2$) and ^{107,109}Ag nuclei ($I = 1/2$), and further correlation between these doublets is established *via* strong $^2J(^{31}P,^{31}P)$ coupling in which each ^{31}P doublet is also scalar coupled to the other ^{31}P doublet, thus yielding complicated fine structure. A more detailed and complete analysis of the coupling is obtained from the ^{31}P 2-D CPCOSY spectra of Fig. 5, and values of all ^1J(Ag,P) and most ^2J(P,P) coupling constants can be determined. The ^{31}P NMR parameters measured from these spectra are listed in Table 4.

The ^{31}P CPMAS spectra of $[Ag_2(PPh_3)_4(SO_4)]\cdot 2H_2O$ at 9.40 and 17.62 T shown in Fig. 4(a) appear as a single AMX-type multiplet. This is contrary to the result of the crystal structure determination which suggests that 4 inequivalent phosphorus sites should exist. There was no detectable change to the ^{31}P CPMAS spectrum of **1** upon reduction of the sample temperature to 200 K (*i.e.* the temperature at which X-ray structural analyses were performed), which confirmed that dynamic processes were not responsible for averaging any part of the spectrum at the higher ambient temperatures. The fact that ^2J(P,P) coupling is evident means that the observed 'equivalence' (or accidental overlap of chemical shifts) of the P atoms involves those attached to *different* silver centres, so that the two P_2Ag units comprising the dimer 'appear' equivalent, although this is not dictated by crystal symmetry. The 17.62 T spectrum did not result in further resolution of the signals, but broader lines and reduced resolution of the ^2J(P,P) coupling in the multiplet at δ 16.7 suggest a marginally greater chemical shift separation for the two phosphorus sites giving rise to this signal. The situation for $[Ag_2(PPh_3)_4(SeO_4)]\cdot 2H_2O$, which is isostructural with **1**, is a marked contrast where the complex spectra at 9.40 and 17.72 T (see Fig. 4(b)) consist of two overlapping AMX multiplets (*i.e.* 4 doublets of doublets). Here the multiplet structure from each site is sufficiently chemically shifted to be almost completely resolved. It is interesting from Fig. 4(a) and (in particular) 4(b) that although greater chemical shift dispersion (in hertz) is introduced at 17.62 T, the intrinsic resolution defining the ^1J(Ag,P) and ^2J(P,P) structure is reduced, a phenomenon that has been attributed to bulk susceptibility broadening.[28] The ^{31}P 2-D CPCOSY results at 9.40 T of complexes **1** and **2** shown in Fig. 5(a) and (b) substantiate the above observations. The CPCOSY spectrum for $[Ag_2(PPh_3)_4(SeO_4)]\cdot 2H_2O$ clearly displays all 16 resonances to be fully resolved as off-diagonal correlations, while that for $[Ag_2(PPh_3)_4(SO_4)]\cdot 2H_2O$ shows only a single multiplet exhibiting off-diagonal correlations which are diffuse and poorly resolved. Furthermore, the latter spectrum shows evidence of additional correlations on the high-field side of the primary multiplet structure, indicating the presence of further multiplet structure. This is consistent with the presence of two P_2Ag units that are only very slightly chemically shifted with respect to each other.

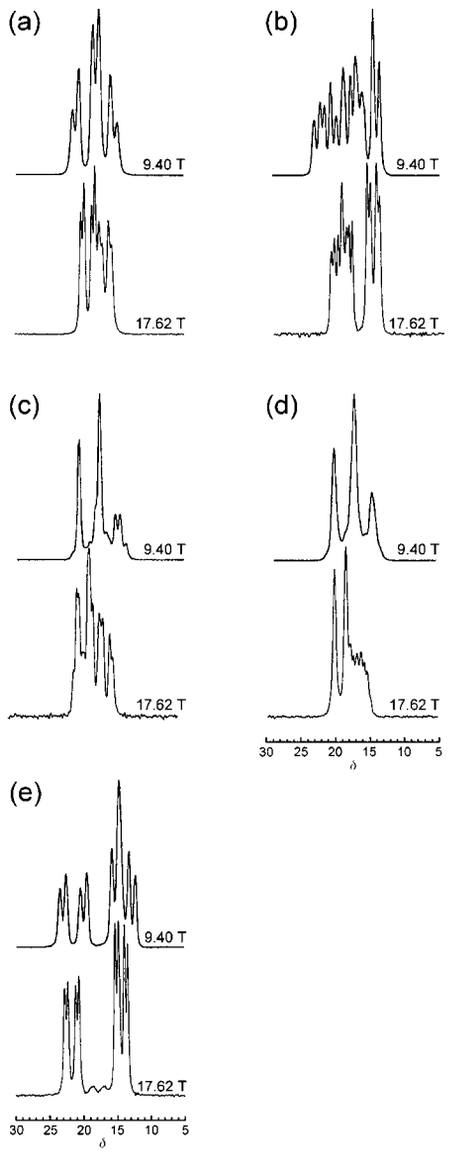

Fig. 4 Solid-state ^{31}P CPMAS NMR spectra acquired at 9.40 and 17.62 T of (a) $[Ag_2(PPh_3)_4(SO_4)]\cdot 2H_2O$ **1**, (b) $[Ag_2(PPh_3)_4(SeO_4)]\cdot 2H_2O$ **2**, (c) $[Ag(PPh_3)_2(HSO_4)]\cdot H_2O$ **3**, (d) $[Ag(PPh_3)_2(HSeO_4)]\cdot H_2O$ **4** and (e) $[Ag(PPh_3)_2(H_2PO_4)]\cdot 2EtOH$ **5**. All chemical shifts are relative to solid PPh_3.

Table 4 Solid-state CPMAS ^{31}P NMR parameters

Complex	$\delta(^{31}P)^a$	^1J(Ag,P)/Hz	^2J(P,P)/Hz
$[Ag_2(PPh_3)_4(SO_4)]\cdot 2H_2O$	16.7 ± 0.2	453 ± 10	148 ± 5
	19.6 ± 0.2	492 ± 10	148 ± 5
$[Ag_2(PPh_3)_4(SeO_4)]\cdot 2H_2O$	15.4 ± 0.1	352 ± 5	148 ± 3
	21.5 ± 0.1	531 ± 5	148 ± 3
	15.5 ± 0.1	414 ± 5	148 ± 3
	20.1 ± 0.1	484 ± 5	148 ± 3
$[Ag(PPh_3)_2(HSO_4)]\cdot H_2O$	15.6 ± 0.2	469 ± 10	148 ± 5
	17.4 ± 0.2	484 ± 10	148 ± 5
	19.2 ± 0.3	492 ± 10	—
$[Ag(PPh_3)_2(HSeO_4)]\cdot H_2O$	16.7 ± 0.3	437 ± 15	—
	19.5 ± 0.3	488 ± 15	—
$[Ag(PPh_3)_2(H_2PO_4)]\cdot 2EtOH$	14.1 ± 0.1	406 ± 5	148 ± 3
	21.6 ± 0.1	492 ± 5	148 ± 3
	14.8 ± 0.1	—	—

[a] Relative to solid PPh_3.

The 1- and 2-D spectra of $[Ag(PPh_3)_2(HSO_4)]\cdot H_2O$ (see Figs. 4(c) and 5(c)) are assigned as a superposition of 2 ABX

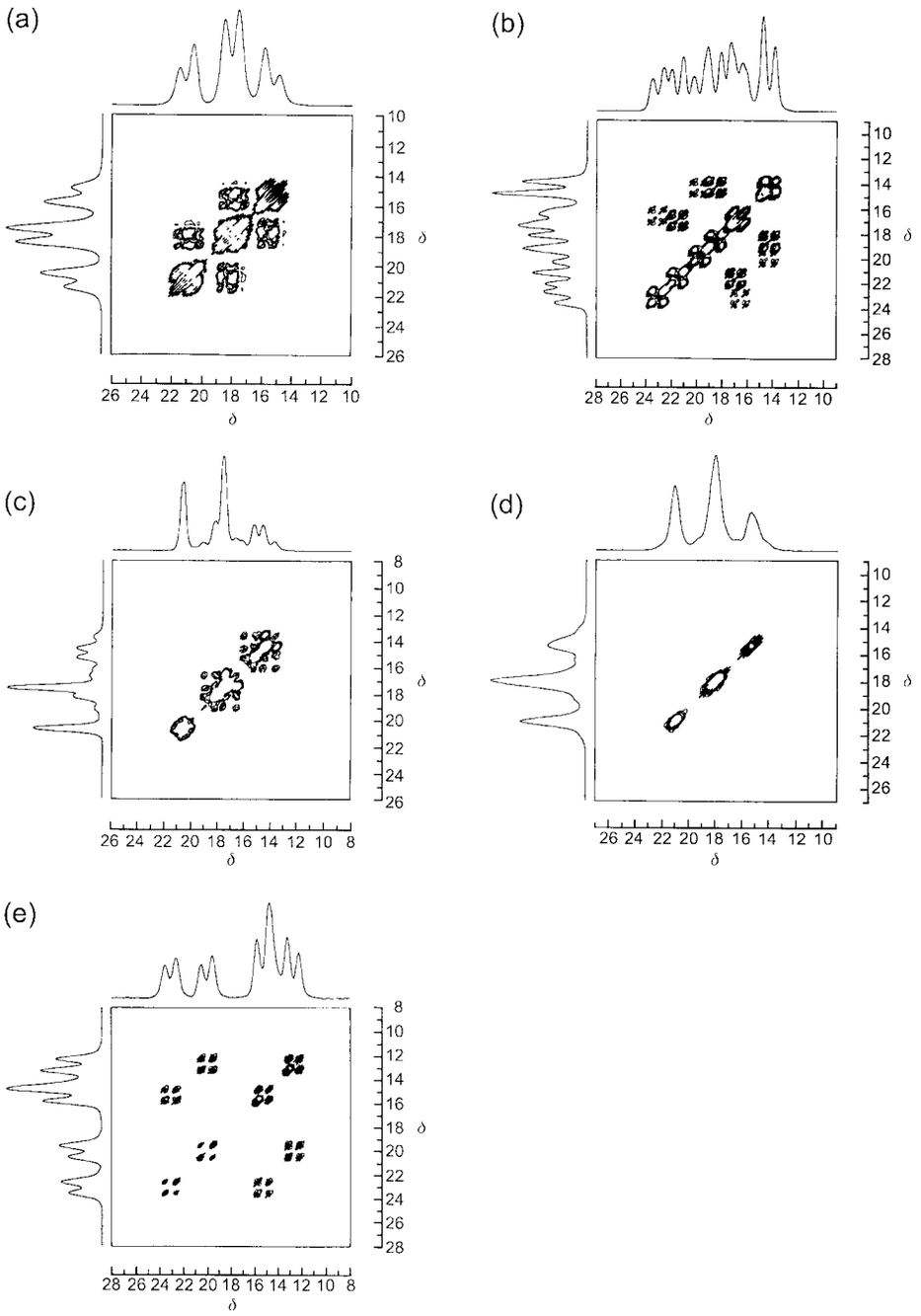

Fig. 5 Solid-state ^{31}P 2-D CPCOSY spectra acquired at 9.40 T of complexes **1**–**5**. Details as in Fig. 4.

multiplets. The more strongly coupled ABX multiplet at lower field ($\delta \approx 19.2$) gives the appearance at 9.40 T of an A_2X pattern, but at very high field some partially resolved ^2J(P,P) fine structure emerges, confirming its ABX nature. The more weakly coupled ABX multiplet at higher field (based around shifts of δ 15.6 and 17.4) is responsible for the more resolved structure evident at both fields This is consistent with the crystal structure of complex **3** as depicted in Fig. 2, which exhibits two quite different monomeric P_2Ag moieties in the unit cell. The closeness of the Ag–P bond distances given in Table 2 suggests that both P_2Ag moieties should exhibit near chemical equivalence in the ^{31}P multiplets, with the $P_2Ag(2)$ moiety expected to produce the more nearly equal chemical shifts. Thus, the lower field multiplet is assigned to this unit. From the ^{31}P 2-D CPCOSY data of Fig. 5(c) the ABX sub-spectrum of the $P_2Ag(1)$ moiety produces ^2J(P,P) coupling which is readily observed as off-diagonal correlations located very close to the main diagonal. The 1-D spectrum of $[Ag(PPh_3)_2(HSeO_4)]\cdot H_2O$ at 9.40 T (see Fig. 4(d)) is similar in appearance to that of its HSO_4 analogue, but in this case both multiplets closely resemble A_2X-type manifolds. The CPCOSY spectrum of Fig. 5(d) at this field shows that no off-diagonal correlations exist, confirming that both P_2Ag moieties may be described as strongly coupled A_2X spin systems. However, the 17.62 T spectrum (see Fig. 4(d)) shows that only the low field multiplet at δ 19.5 is a true A_2X spin system, while the higher field multiplet at $\delta \approx 16.7$ is more accurately described as an ABX system with partially resolved ^2J(P,P) structure now being observed. The A_2X multiplet (doublet) at δ 19.5 is assigned to the $P_2Ag(2)$ moiety because of the near equality of the two Ag–P bond lengths for this unit (Table 2).

The spectra of $[Ag(PPh_3)_2(H_2PO_4)]\cdot 2EtOH$ shown in Fig. 4(e) consist of a single resonance due to the H_2PO_4 phosphorus atom, and a superimposed AMX multiplet due to the P_2Ag unit. Coupling correlations in this latter system are clearly evident in the corresponding CPCOSY spectrum of Fig. 5(e).

The ^1J(Ag,P) coupling constants in Table 4 cover a wide range, from 352 to 531 Hz. It has previously been shown that

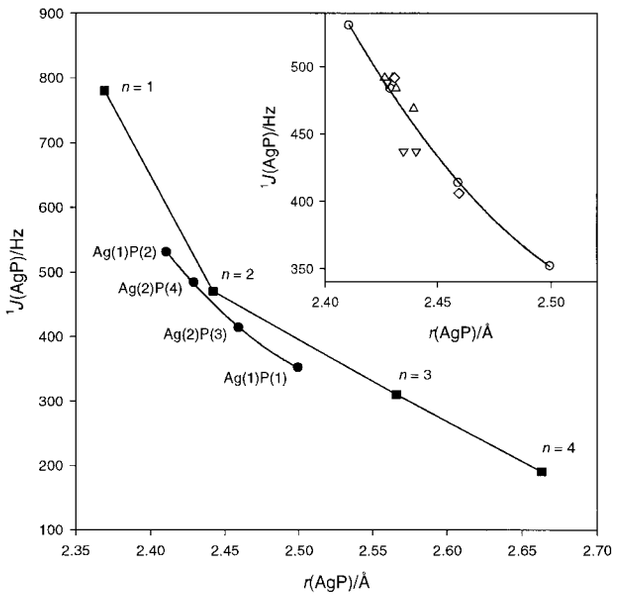

Fig. 6 Plot of ^1J(Ag,P) *vs.* the Ag–P bond length *r*(AgP) for $[Ag_2(PPh_3)_4(SeO_4)]\cdot 2H_2O$ (●) and $[Ag(PPh_3)_n(NO_3)]$ ($n = 1$–4) (■). Inset: best fit curve for $[Ag_2(PPh_3)_4(SeO_4)]\cdot 2H_2O$ (○), with data for $[Ag(PPh_3)_2(HSO_4)]\cdot H_2O$ (△), $[Ag(PPh_3)_2(HSeO_4)]\cdot H_2O$ (▽) and $[Ag(PPh_3)_2(H_2PO_4)]\cdot 2EtOH$ (◇).

one of the factors that determines the magnitude of ^1J(M,P) coupling constants in metal–phosphine complexes is the number of phosphine ligands coordinated.[29–33] The averages of the two ^1J(Ag,P) coupling constants for the various P_2Ag groups in the compounds listed in Table 4 lie in the range 440–490 Hz, and these values are similar to those reported previously for other silver complexes containing an oxyanion and two coordinated PPh_3.[5,29] However, it is clear from the results in Table 4 that the ^1J(Ag,P) values of compounds with a fixed number of coordinated phosphines still cover a considerable range, suggesting that other factors are also important in determining the magnitude of this parameter. An obvious factor is the strength of the Ag–P bond, which is reflected in the Ag–P bond length; $[Ag_2(PPh_3)_4(SeO)_4]\cdot 2H_2O$ is a unique example which provides four completely resolved coupling constants from four Ag–P bonds of different length in a single compound. For this complex it was possible to resolve all four ^{31}P chemical shifts, and an analysis of the multiplet positioning in the 2-D CPCOSY spectrum facilitates assignment of pairs of ^1J(Ag,P) values unambiguously to one of the two Ag atoms in the structure. With the additional assumption that the larger of the two coupling constants is associated with the shorter of the two bonds, the plot of ^1J(Ag,P) *vs.* the bond length *r*(AgP) shown in Fig. 6 is obtained. It is noted that this assumption gives the internally consistent result that Ag(1), which exhibits the larger difference in *r*(AgP), also exhibits the larger difference in ^1J(Ag,P) values in comparison to Ag(2). Also shown in Fig. 6 is a plot of ^1J(Ag,P) *vs.* *r*(AgP) for $[Ag(PPh_3)_n(NO_3)]$ ($n = 1$–4) using previously reported data.[29] From this it is clear that the dependence of ^1J(Ag,P) on bond length is similar for the two different types of compound. Furthermore, the data for $[Ag(PPh_3)_2(HSO_4)]\cdot H_2O$, $[Ag(PPh_3)_2(HSeO_4)]\cdot H_2O$ and $[Ag(PPh_3)_2(H_2PO_4)]\cdot 2EtOH$ all lie very close to the curve for $[Ag_2(PPh_3)_4(SeO_4)]\cdot 2H_2O$ in Fig. 6. It is noteworthy that $[Ag_2(PPh_3)_4(SO_4)]\cdot 2H_2O$, which shows almost identical Ag–P bond lengths to those of the selenate analogue, does not show the same range of ^1J(Ag,P) values, due to the unexpected near equivalence of the two P_2Ag units as described above.

Vibrational spectroscopy

The mid-range IR spectra (4000–400 cm^{-1}) of complexes **1**–**5** contain bands due to the coordinated oxyanions, together with

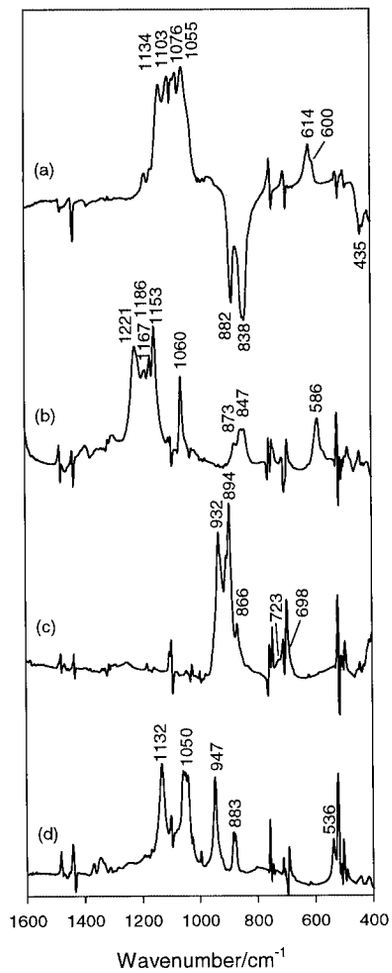

Fig. 7 Mid-range IR difference spectra showing bands due to the oxyanions in (a) $[Ag_2(PPh_3)_4(SO_4)]\cdot 2H_2O/[Ag_2(PPh_3)_4(SeO_4)]\cdot 2H_2O$, (b) $[Ag(PPh_3)_2(HSO_4)]\cdot H_2O$, (c) $[Ag(PPh_3)_2(HSeO_4)]\cdot H_2O$ and (d) $[Ag(PPh_3)_2(H_2PO_4)]\cdot 2EtOH$. Spectrum (a) was obtained by subtraction of the selenate spectrum from the sulfate spectrum; positive bands are due to sulfate and negative bands to selenate. Spectra (b)–(d) were obtained by subtracting the spectrum of coordinated PPh_3 (see text). The unlabelled features are residuals of the much stronger PPh_3 bands in the original spectra.

many bands due to the PPh_3 ligand. The presence of the latter bands interferes with the assignment of the oxyanion bands, but it is possible to minimize this interference by means of spectral subtraction. This was done in two ways, the results of which are shown in Fig. 7. For the sulfate and selenate compounds, direct subtraction of the spectrum of **2** from that of **1** results in almost complete elimination of the bands due to coordinated PPh_3, leaving bands due to the SO_4^{2-} and SeO_4^{2-} ions as positive and negative features respectively (Fig. 7(a)). The same method worked reasonably well for **3** and **4**, but because of partial overlap of the HSO_4^- and $HSeO_4^-$ bands an alternative method was adopted which was also applicable to the $H_2PO_4^-$ complex **5**. This method involves extraction of the spectrum of coordinated PPh_3 from the spectrum of the selenate complex **2**, where the overlap of the oxyanion and PPh_3 bands is minimal, and subtracting this from the spectra of the complexes **3**–**5** (Fig. 7(b)–(d)).

The wavenumbers of the bands assigned to vibrations of the oxyanions are compared with those for the uncomplexed oxyanions[34–36] in Table 5. The symmetry types and activities of the normal modes of the free EO_4^{n-} species (point group symmetry T_d) are $A_1(R) + E(R) + 2T_2(IR, R)$. The binding of a proton to these ions causes considerable band shifts and splittings, as is evident in the spectra of HSO_4^- (Table 5). The most significant effect of protonation is a lowering of the

Table 5 Wavenumbers (cm^{-1}) of the vibrations of the EO_4 (E = S, Se or P) groups in complexes **1**–**5**,[a] and of the correspondng uncomplexed oxyanions

Compound	$\nu_1(A_1)$	$\nu_3(T_2)$	$\nu_2(E)$	$\nu_4(T_2)$
$[Ag_2(PPh_3)_4(SO_4)]\cdot 2H_2O$ **1**	942(R)	1134, 1103, 1076, 1055		614, 600
$[Ag_2(PPh_3)_4(SeO_4)]\cdot 2H_2O$ **2**	818(R)	882, 838	357	435
$[Ag(PPh_3)_2(HSO_4)]\cdot H_2O$ **3**	1060	1221, 1186, 1167, 1153, 873, 847		586
$[Ag(PPh_3)_2(HSeO_4)]\cdot H_2O$ **4**	866, 860(R)	932, 894, 723, 698	328	389
$[Ag(PPh_3)_2(H_2PO_4)]\cdot 2EtOH$ **5**	1050, 1045(R)	1132, 947, 883, 876	378	536
SO_4^{2-} [b]	983	1105	450	611
SeO_4^{2-} [b]	833	875	335	432
HSO_4^- [c]	1040	1195, 895	411	594
$HSeO_4^-$ [d]	866	921, 743	324	396
$H_2PO_4^-$ [e]	1070	1150, 945, 880	393, 360	515

[a] IR bands are unlabelled; Raman bands are labelled (R). [b] Ref. 31. [c] Ref. 32. [d] This work, measured from the Raman spectrum of a *ca.* 4 mol L^{-1} aqueous solution of $KHSeO_4$. [e] Ref. 33.

frequency of one of the T_2 ν(E–O) modes, and these lower frequency modes are described as ν(E–OH) modes, being mainly due to a ν(E–O) vibration involving the protonated oxygen atom. Thus, the ν(S–OH) band of HSO_4^- is assigned at 895 cm^{-1}.[35] Similarly, two ν(P–OH) bands occur for $H_2PO_4^-$, at 945, 880 cm^{-1}.[36] It is evident from the results in Table 5 that, although coordination of these oxyanions to silver causes some perturbation of the anion vibrations, the bands do not shift very far from those of the uncomplexed parent anions, and can be assigned on the same basis. For the sulfate and selenate complexes **1** and **2**, the T_2 ν(E–O) band ν_3 is split due to the low symmetry environment of the anion in these complexes (Fig. 1), and the average frequency of the band is slightly lower than that of the free anion. For the hydrogen-sulfate and -selenate compounds **3** and **4**, the ν(E–O) bands derived from ν_3 of the parent EO_4^{2-} cover a much wider range than in **1** and **2**, but these bands can readily be assigned on the basis of the assignments discussed above for HSO_4^-. Thus, the band at about 850 cm^{-1} for **3** correlates with ν(S–OH) at 895 cm^{-1} for HSO_4^-, the frequency again being lowered by coordination to silver. The group of bands around 1200 cm^{-1} correlates with ν(S–O) at 1195 cm^{-1} for HSO_4^-. This mode, which has E symmetry in the free ion (point group C_{3v}),[35] is split due to the lower symmetry environment and the presence of two inequivalent sites for the ion in the complex (Fig. 2). The band at 1060 cm^{-1} correlates with the band at 1040 cm^{-1} of HSO_4^-, which has been described as the totally symmetric ν(S–O) stretch in the free ion.[35] Similar bands to those of **3** are observed for the hydrogenselenate complex **4** (Table 5). The assignments of the PO_4 group vibrations in the dihydrogenphosphate complex **5** follows readily from those of free $H_2PO_4^-$ (Table 5).

The bands in the Raman spectra due to the oxyanions are much weaker than those of triphenylphosphine, and only those that derive from $\nu_1(A_1)$ of the EO_4 groups were identified (Table 5).

The far-IR spectra of complexes **1**–**5** are shown in Fig. 8. By analogy with results for formate complexes $[M(PPh_3)_n(O_2CH)]$ (M = Cu or Ag; $n = 2$ or 3), ν(Ag–O) modes are expected to occur below 300 cm^{-1}.[5,6] All of the spectra show a weak, relatively sharp band at about 210 cm^{-1} which is attributed to the PPh_3 ligand, together with weak, broader bands (or multiple bands) in the 150–300 cm^{-1} region which are possibly due to ν(Ag–O). This is consistent with a shift in the position of the band from approximately 200 cm^{-1} for the hydrogen-sulfate complex **3** to about 260 cm^{-1} for the dihydrogen-phosphate complex **5** (Fig. 8), since a shorter (and therefore stronger) Ag–O bond is observed in this complex (2.328 Å, Table 3) relative to **3** (2.410 Å, Table 2). We therefore assign these bands as ν(Ag–O) modes, although some uncertainty remains because of their low intensity. The far-IR spectra of Ag_3PO_4 and Ag_2HPO_4 were also recorded, and these show strong ν(Ag–O) bands at 202 and 234 cm^{-1} respectively. Given that the bonding modes for the anions are different (quadruple

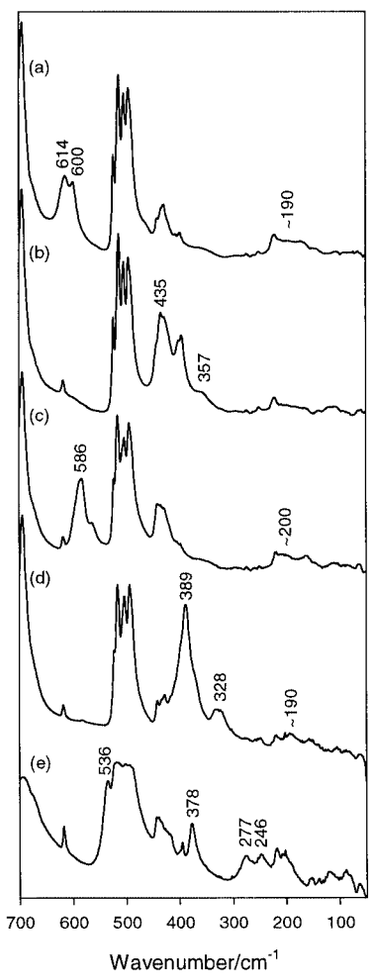

Fig. 8 Far-IR spectra of (a) $[Ag_2(PPh_3)_4(SO_4)]\cdot 2H_2O$, (b) $[Ag_2(PPh_3)_4(SeO_4)]\cdot 2H_2O$, (c) $[Ag(PPh_3)_2(HSO_4)]\cdot H_2O$, (d) $[Ag(PPh_3)_2(HSeO_4)]\cdot H_2O$ and (e) $[Ag(PPh_3)_2(H_2PO_4)]\cdot 2EtOH$.

bridging in Ag_3PO_4,[37] terminal in **5**), and that bridging bond vibrations normally occur at lower frequencies than terminal bond vibrations, these assignments are quite consistent with ν(Ag–O) ≈ 260 cm^{-1} in **5**.

The present vibrational results for the coordinated oxyanions EO_4^{n-} in their unprotonated and partially protonated forms provide information that may assist in identification of these anions in related bonding situations. Thus, a surface-enhanced Raman spectroscopy (SERS) study of the adsorption of PO_4^{3-} and HPO_4^{2-} ion on silver resulted in the assignment of ν(Ag–O) at 230 and 240 cm^{-1} respectively,[18] quite close to the value of *ca.* 260 cm^{-1} observed in the present study for the $H_2PO_4^-$ complex **5**. In many of the studies of sulfate on metal surfaces, there is some uncertainty about whether the adsorbed species is SO_4^{2-}

or HSO_4^-.[12,14,16,17,38–43] This is rather surprising in view of the results described herein, which show that the effect of a bound proton on the SO_4 vibrations is much greater than that of an attached metal atom, so that a distinction between SO_4^{2-} and HSO_4^- on the basis of vibrational spectroscopy should be possible. In particular, the strong activation of the $\nu_1(A_1)$ band in the IR, and the presence of a low frequency ν(S–OH) IR band should be diagnostic of HSO_4^-.

Acknowledgements

G. A. B. and J. V. H. would like to thank the Australian Institute of Nuclear Science and Engineering (AINSE) for funding of AINSE Project No. 00/011. The very high field (17.6 T) NMR data presented were collected in the Environmental Molecular Sciences Laboratory, a national scientific user facility sponsored by the Department of Energy's Office of Biological and Environmental Research and located at the Pacific Northwest National Laboratory.

References

1 R. J. Lancashire, *Comprehensive Coordination Chemistry*, ed. G. Wilkinson, Pergamon, Oxford, 1987, vol. 5, p. 775.
2 C. E. Holloway, M. Melnik, W. A. Nevin and W. Liu, *J. Coord. Chem.*, 1995, **35**, 85.
3 A. Angel and A. V. Harcourt, *J. Chem. Soc.*, 1902, **81**, 1385.
4 A. Angel, *J. Chem. Soc.*, 1906, **89**, 345.
5 G. A. Bowmaker, Effendy, J. V. Hanna, P. C. Healy, G. J. Millar, B. W. Skelton and A. H. White, *J. Phys. Chem.*, 1995, **99**, 3909.
6 G. A. Bowmaker, Effendy, J. V. Hanna, P. C. Healy, J. C. Reid, C. E. F. Rickard and A. H. White, *J. Chem. Soc.*, *Dalton Trans.*, 2000, 753.
7 L. Coghi and G. Pelizzi, *Acta Crystallogr.*, *Sect. B*, 1975, **31**, 131.
8 A. Stiewe, E. Kemnitz and S. Troyanov, *Z. Anorg. Allg. Chem.*, 1999, **625**, 329.
9 J. A. R. Navarro, M. A. Romero, J. M. Salas, R. Faure and X. Solans, *J. Chem. Soc.*, *Dalton Trans*, 1997, 2321.
10 J. A. R. Navarro, J. M. Salas, M. A. Romero and R. Faure, *J. Chem. Soc.*, *Dalton Trans.*, 1998, 901.
11 M.-L. Tong, S.-L. Zheng and X.-M. Chen, *Chem. Commun.*, 1999, 561.
12 O. R. Melroy, M. G. Samant, G. L. Borges, J. G. Gordon, L. Blum, J. H. White, M. J. Albarelli, M. McMillan and H. D. Abruna, *Langmuir*, 1988, **4**, 728; M. F. Toney, J. N. Howard, J. Richer, G. L. Borges, J. G. Gordon, O. R. Melroy, D. Yee and L. B. Sorensen, *Phys. Rev. Lett.*, 1995, **75**, 4472.
13 A. Tadjeddine, D. Guay, M. Ladouceur and G. Tourillon, *Phys. Rev. Lett.*, 1991, **66**, 2235.
14 O. M. Magnussen, J. Hageböck, J. Hotlos and R. J. Behm, *Faraday Discuss. Chem. Soc.*, 1992, **94**, 329.
15 Z. Shi and J. Lipkowski, *J. Electroanal. Chem.*, 1994, **365**, 303.
16 G. J. Edens, X. Gao and M. J. Weaver, *J. Electroanal. Chem.*, 1994, **375**, 357.
17 H. Uchida, M. Hiei and M. Watanabe, *J. Electroanal. Chem.*, 1998, **452**, 97.
18 G. Niaura, A. K. Gaigalas and V. L. Vilker, *J. Phys. Chem. B*, 1997, **101**, 9250.
19 G. A. Bowmaker, Effendy, J. V. Hanna, P. C. Healy, B. W. Skelton and A. H. White, *J. Chem. Soc.*, *Dalton Trans.*, 1993, 1387.
20 J. V. Hanna and S. W. Ng, *Acta Crystallogr.*, *Sect. C*, 2000, **56**, 24.
21 G. M. Sheldrick, SHELX 97, Program for Refinement of Crystal Structures, University of Göttingen, 1997.
22 A. Pines, M. G. Gibby and J. S. Waugh, *J. Chem. Phys.*, 1973, **59**, 569.
23 E. R. Andrew, A. Bradbury and R. Eades, *Nature* (*London*), 1958, **182**, 1659.
24 E. O. Stejskal and J. Schaefer, *J. Magn. Reson.*, 1975, **18**, 560.
25 G. Bodenhausen, R. L. Vold and R. R. Vold, *J. Magn. Reson.*, 1980, **37**, 93; D. Marion and K. Wuthrich, *Biochem. Biophys. Res. Commun.*, 1983, **113**, 967; T. Allman, *J. Magn. Reson.*, 1989, **83**, 637.
26 J. V. Hanna, M. E. Smith, S. N. Stuart and P. C. Healy, *J. Phys. Chem.*, 1992, **96**, 7560.
27 P. Gilli, V. Bertolasi, V. Ferretti and G. Gilli, *J. Am. Chem. Soc.*, 1994, **116**, 909.
28 G. Wu and R. E. Wasylishen, *Organometallics*, 1992, **11**, 3242.
29 P. F. Barron, J. C. Dyason, P. C. Healy, L. M. Engelhardt, B. W. Skelton and A. H. White, *J. Chem. Soc.*, *Dalton Trans.*, 1986, 1965.
30 S. Attar, N. W. Alcock, G. A. Bowmaker, J. S. Frye, W. H. Bearden and J. H. Nelson, *Inorg. Chem.*, 1991, **30**, 4166.
31 L. J. Baker, G. A. Bowmaker, D. Camp, Effendy, P. C. Healy, H. Schmidbaur, O. Steigelmann and A. H. White, *Inorg. Chem.*, 1992, **31**, 3656.
32 E. C. Alea, J. Malito and J. H. Nelson, *Inorg. Chem.*, 1987, **26**, 4294.
33 E. L. Muetterties and C. W. Alegranti, *J. Am. Chem. Soc.*, 1972, **94**, 6386.
34 K. Nakamoto, *Infrared and Raman Spectra of Inorganic and Coordination Compounds*, Fifth Edition, Wiley, New York, 1997, Part A, p. 199.
35 Z. Mielke and H. Ratajczak, *J. Mol. Struct.*, 1973, **18**, 493; R. J. Gillespie and E. A. Robinson, *Can. J. Chem.*, 1962, **40**, 644; D. J. Turner, *J. Chem. Soc.*, *Faraday Trans. 2*, 1972, **68**, 643.
36 E. Stenger and K. Herzog, *Z. Anorg. Allg. Chem.*, 1964, **331**, 169.
37 L. Helmholz, *J. Chem. Phys.*, 1936, **4**, 316.
38 M. G. Samant, K. Kunimatsu, H. Seki and M. R. Philpott, *J. Electroanal. Chem. Interfacial Electrochem.*, 1990, **280**, 391; D. B. Parry, M. G. Samant, H. Seki, M. R. Philpott and K. Ashley, *Langmuir*, 1993, **9**, 1878.
39 P. W. Faguy, N. Markovic, R. R. Adzic, C. A. Fierro and E. B. Yeager, *J. Electroanal. Chem. Interfacial Electrochem.*, 1990, **289**, 245; P. W. Faguy, N. S. Marinkovic and R. R. Adzic, *J. Electroanal. Chem.*, 1996, **407**, 209.
40 Y. Shingaya and M. Ito, *J. Electroanal. Chem.*, 1994, **372**, 283; I. Oda, Y. Shingaya, H. Matsumoto and M. Ito, *J. Electroanal. Chem.*, 1996, **409**, 95; Y. Shingaya, K. Hirota, H. Ogasawara and M. Ito, *J. Electroanal. Chem.*, 1996, **409**, 103.
41 G. M. Brown and G. A. Hope, *J. Electroanal. Chem.*, 1995, **382**, 179.
42 M. Weber and F. C. Nart, *Langmuir*, 1996, **12**, 1895.
43 Y. Sawatari, J. Inukai and M. Ito, *J. Electron Spectrosc. Relat. Phenom.*, 1993, **64/65**, 515.